

飞秒激光刻写布拉格光栅反射光谱特性研究

董欣然¹, 王子安¹, 曾理^{2,3}, 孙小燕^{2,3*}¹中南林业科技大学机电工程学院, 湖南长沙 410018;²中南大学机电工程学院, 湖南长沙 410083;³中南大学高性能复杂制造国家重点实验室, 湖南长沙 410083

摘要 利用飞秒激光相位掩模加工方法制造光纤布拉格光栅(FBG),并研究了激光能量和曝光时间对FBG波长、反射率和带宽的影响规律。研究发现,随着曝光时间的增加,光纤的折射率调制量逐渐变大,耦合效率增大,反射率逐渐变大。当光纤耦合效率达到饱和时,反射率保持不变;当过曝光时,反射率轻微减小,光纤的平均有效折射率和折射率调制深度均变大,带宽增大。随着激光能量的增大,达到最大反射率所需要的曝光时间缩短,且FBG波长的红移量越多,带宽就越大。过大的激光能量会使平均有效折射率和折射率调制深度变大,从而导致FBG主谐振峰两边的旁瓣增多,影响光谱质量。另外,短波方向旁瓣的振荡比较显著,而长波方向则比较平顺。因此,在实际加工中需要选择合适的激光曝光能量和曝光时间。实验获得的最大FBG反射强度达到15 dB,且其光谱变化和理论分析一致。该研究为高质量FBG的制造和光谱特性优化提供了实验依据。

关键词 光纤光学; 光纤布拉格光栅; 飞秒激光; 相位掩模法; 光谱特性; 带宽

中图分类号 TN2 **文献标志码** A

DOI: 10.3788/CJL221198

1 引言

1978年,Hill等^[1]将488 nm氩离子激光注入到掺锗光纤中,首次在纤芯内部观察到入射光与反射光形成的干涉条纹场,发现了光纤的光敏特性,并制造了世界上第一个光纤布拉格光栅器件。光纤布拉格光栅(FBG)作为一种典型的无源光器件,除了具有光纤器件抗电磁干扰能力强、耐腐蚀等优点外,还具有结构尺寸小、反射式操作、灵敏度高、波长编码、波分复用能力强等独特优点^[2-4],在温度^[5-7]、应变^[8-9]、折射率^[10-11]等光纤传感领域备受关注。

FBG器件的制造主要采用直写法^[12-14]、相位掩模法^[15-16]、双光束干涉法^[17]和双光子聚合法^[18]。在直写法中,光栅周期等刻写参数灵活可控,适用于制造不同类型FBG器件。但是,加工系统构建需要高精度位移平台和高倍聚焦系统,相对复杂且加工效率低。在相位掩模法中,光栅周期等参数受限于掩模板的设计参数,但是光栅质量好,器件一致性和稳定性好,加工效率高,适用于光栅的大批量生产,是目前最有前景的技术方案。

传统方法刻写FBG主要采用紫外激光光源,为了增加光纤材料对激光的吸收率,需要预先对光纤进行载氢处理,刻写的光栅热稳定性差,在500℃时会发生

不可逆的光栅擦除^[19]。飞秒激光具有极高的峰值功率和极短的脉冲宽度,与光纤材料作用时表现出较强的非线性效应^[20-21],加工的FBG器件具有折射率调制量大、光纤无需载氢处理、光栅可耐受1000℃高温且热稳定性好等优点^[22-23]。飞秒激光刻写的光栅在高温测量、高温应变等领域中展现出无可替代的优势。2008年,Li等^[24]研究了相位掩模法加工载氢和非载氢FBG的光谱特性和热处理性质,结果显示,在载氢处理的光纤上制造的FBG具有更优异的光谱特性,但是热稳定性没有显著变化。目前,研究者主要关注飞秒激光刻写FBG器件的相关传感特性及传感规律,而关于FBG器件光谱特性的研究相对较少,且缺乏飞秒激光相位掩模法制造FBG器件光谱特性演变规律的完备论述。FBG光谱特性直接影响器件的传感特性,因此FBG光谱特性的研究具有重要的意义。

本文构建了飞秒激光相位掩模法制造FBG器件的系统,并系统研究了曝光时间和激光能量对FBG反射光谱(包括波长、反射率、带宽和光谱边缘质量等)的影响规律。研究发现:随着曝光时间的增加,FBG的反射率逐渐增加,最后保持不变,波长也会发生轻微红移;随着激光能量的增加,达到最大反射率所需要的时间缩短;激光能量的增加会增大光谱带宽,也会使主谐振峰的旁瓣增加。因此,为了获得最

收稿日期: 2022-09-01; 修回日期: 2022-09-29; 录用日期: 2022-10-11; 网络首发日期: 2022-11-04

基金项目: 国家自然科学基金青年基金(52005521)、湖南省自然科学基金青年基金(2021JJ41079)

通信作者: *sunxy@csu.edu.cn

优的 FBG 光谱,需要确定合适的激光能量和曝光时间。这两个因素是影响相位掩模法制造 FBG 的核心因素。

2 光栅耦合模理论及其加工系统搭建

2.1 光栅耦合模理论分析

光栅模式耦合发生在同向传输的纤芯基模和后向传输的纤芯模式之间,根据耦合模式理论可知,其反射波长(λ_B)的变化^[25]可表示为

$$m\lambda_B = 2n_{\text{eff}}\Lambda, \quad (1)$$

式中: m 表示光栅耦合阶次; n_{eff} 表示光栅的有效折射率; Λ 表示光栅周期。

FBG 的反射率(R)^[26-27]可以表示为

$$R = \tanh^2(\kappa L), \quad (2)$$

式中: κ 表示耦合系数,其大小取决于折射率调制量(Δn_{mod}); L 为光栅长度。

FBG 是弱光栅,其光谱带宽($\Delta\lambda$)^[26]可以表示为

$$\Delta\lambda = \frac{2\lambda_B\Lambda}{L} \sqrt{1 + \left(\frac{\kappa L}{\pi}\right)^2}. \quad (3)$$

由式(2)、(3)可知,FBG 反射率和带宽变化主要取决于光栅耦合效率。

2.2 器件加工系统分析

飞秒激光相位掩模法刻写 FBG 的加工系统如图 1 所示,其中 m 为衍射级数。光栅刻写系统由飞秒激光光源、激光光路、光纤三维精密调整平台、光谱在线监测系统组成。飞秒激光光源主要由种子光源、钛宝石振荡器和再生放大器组成。输出飞秒激光脉冲的中心波长、重复频率和脉冲宽度分别为 800 nm、1 kHz 和 120 fs。激光光路由反射镜、小孔光阑、光衰减片、柱透镜和相位掩模板组成。其中反射镜用于控制激光脉冲的传输方向;光阑用来控制激光光斑大小,改善激光光束边缘质量;光衰减片用来调整激光能量通量大小;柱透镜用于实现激光光束的聚集压缩,提高激光能量密度,其焦距为 50 mm;相位掩模板用于产生

周期性干涉条纹,在标准单模光纤(SMF-28)上写入周期性光栅结构,设计的响应波段和模板周期分别为 1550 nm 和 2142 nm,0 级衍射效率小于 4%,可产生 2 阶 Bragg 响应, ± 1 级衍射角($\theta_{\pm 1}$)为 21.93° ;光纤三维精密调整平台由三维高精度手动位移平台和光纤夹具组成,主要用于调整被加工光纤高度、倾角以及与掩模板之间的相对距离。光谱在线监测系统主要由宽带光源、光纤光谱分析仪、3 dB 耦合器和计算机组成,用于实时监测加工过程中 FBG 反射光谱的变化。其中宽带光源是由上海瀚宇光纤通信有限公司提供的 C+L 波段放大自发辐射(ASE)光源,光纤光谱分析仪测量波长的精度和波长范围分别为 10 pm 和 600~1700 nm。实验中光纤和掩模板之间的距离(d_0)设定为 3 mm,光阑控制入射光斑的半径(W_0)为 4 mm,由干涉条纹长度 $l_0 = 2(W_0 - d_0 \tan \theta_{\pm 1})$ 计算得到, $l_0 = 5.58$ mm,即刻写光栅栅区的长度约为 5.58 mm。

3 结果分析和讨论

实验设定激光曝光能量为 600 mW,重复频率为 1 kHz,不同曝光时间下对应 FBG 反射光谱的变化如图 2(a) 所示。随着激光曝光时间的增加,FBG 反射率逐渐增大,最后基本维持不变,其波长发生红移。当曝光时间从 5 s 增加到 240 s 时,其波长从 1549.33 nm 向长波方向漂移到 1549.69 nm,波长变化量为 0.36 nm,如图 2(b) 所示。FBG 的波长理论上只取决于光栅周期,而光栅周期由相位掩模板周期决定。实验中发现,FBG 波长会发生轻微漂移,这主要是由于随着曝光时间的增加,作用于光纤的激光脉冲数增多,引起光纤的平均有效折射率增加,从而导致波长的变化。如图 2(c) 所示,反射率在初始曝光时迅速增加,在曝光前 20 s 时反射率迅速增加到 11.6 dB,当曝光时间为 75 s 左右时达到最大值,为 14 dB;在曝光 75~130 s 范围内,反射率基本维持不变;当曝光时间持续到 240 s 时,反射率呈现出轻微减小的趋势。这是由于当激光脉冲作用于光纤时,光纤的折射率调制量迅速增加,因此光栅耦合系数增大,反射率增加;在纤芯内部逐渐形成稳定的折射率调制结构,耦合效率趋于稳定,反射率变化也趋于稳定;再持续曝光时,光栅处于过耦合状态,耦合效率反而降低,导致反射率呈现出减小的趋势。由图 2(b)、(c) 可知,FBG 波长和反射率变化与曝光时间的关系都是非线性的。这主要是由于随着曝光时间的增加,飞秒激光脉冲诱导的光纤有效折射率的变化是非线性的^[28]。另外,FBG 带宽随着曝光时间的增加,呈现出增大的趋势,如图 2(d) 所示。在最初曝光 30 s 内 3 dB 带宽迅速增大,而后随着曝光时间的延长,带宽缓慢增加。曝光时间 5、30、100、200 s 条件下对应的带宽分别为 0.41、0.57、0.64、0.74 nm。由式(3)可知,带宽的大小主要取决于光栅的有效折射率变化。实验结果表明,随着曝光时间的

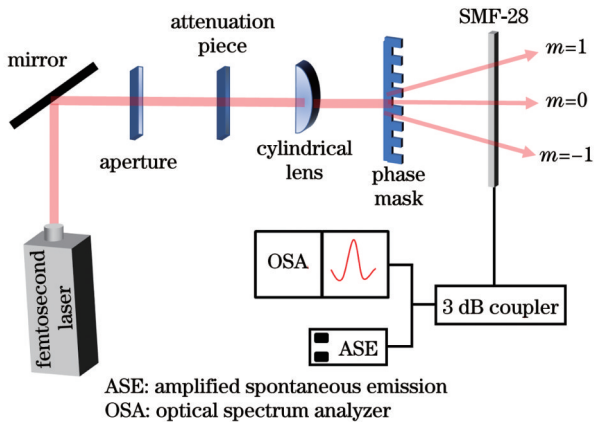


图 1 基于飞秒激光相位掩模法制造 FBG 器件的示意图

Fig. 1 Schematic of FBG fabrication based on femtosecond laser phase mask technology

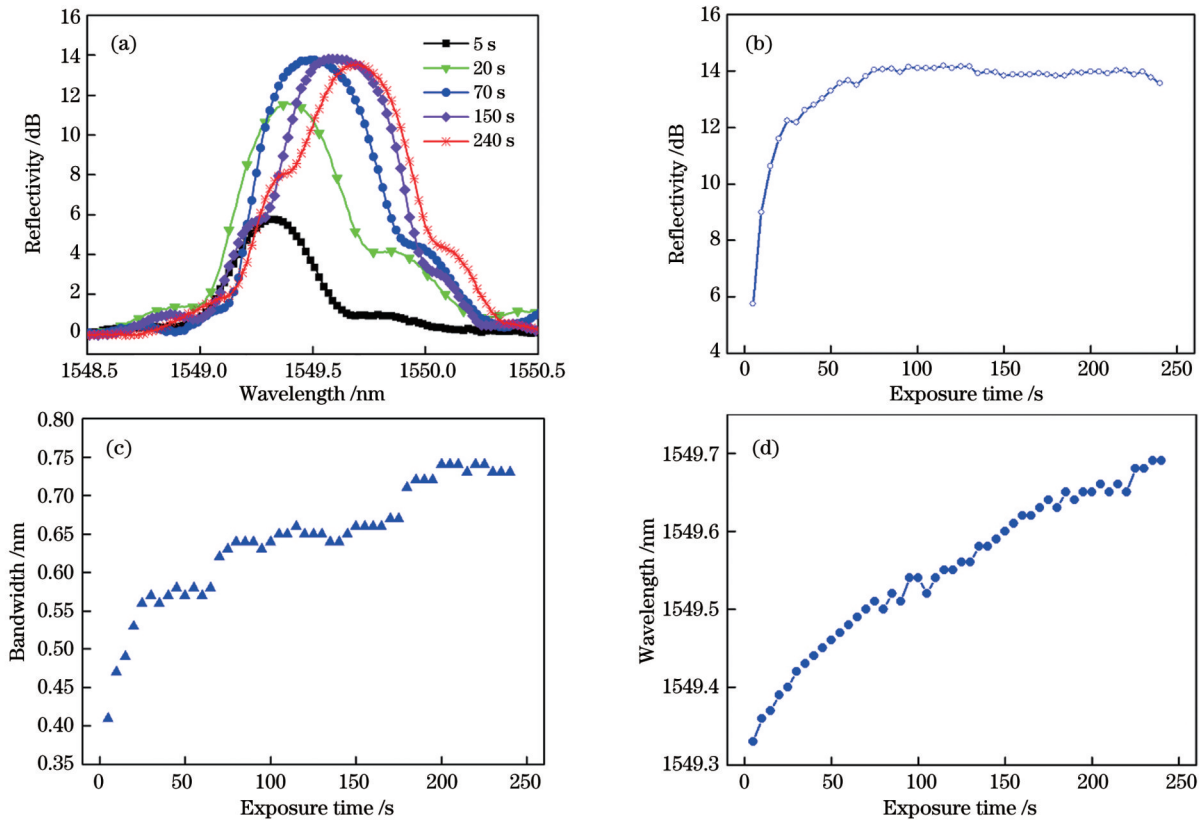


图2 曝光时间对FBG反射光谱的影响。(a)不同曝光时间下的FBG反射光谱;(b)波长、(c)反射率、(d)带宽随曝光时间的变化
Fig. 2 Influence of exposure time on FBG reflectance spectrum. (a) FBG reflectance spectra under different exposure time; (b) wavelength, (c) reflectivity, and (d) bandwidth versus exposure time

增加,飞秒激光诱导光纤有效折射率增大,这一变化趋势与波长的变化趋势相似。综上可知,曝光时间过长不利于获得带宽小的FBG器件,在实际加工中,需要选择最优的曝光时间参数以获得高反射率、低带宽的FBG器件。

此外,实验对比分析了不同激光能量对FBG波长、反射率和带宽等的影响规律,如图3所示。实验发现:在相同曝光时间内,使用的激光能量越大,波长向长波方向的漂移量越大,且波长的增加速率越大,如图3(a)所示。在曝光125 s范围内,激光能量为800 mW时获得的FBG波长漂移量为0.39 nm,显著高于700 mW条件下得到的FBG波长变化量(0.27 nm)。另外,在前30 s范围内,高激光能量下FBG波长的增长速率更大,其波长变化量为0.3 nm,增长速率约为10 pm/s,而当激光能量为700 mW时,波长的变化量为0.2 nm,对应增长速率为6.7 pm/s。这主要是由于激光能量越大,诱导产生的平均有效折射率越大,波长漂移量也越大。此外,随着激光能量的增大,FBG反射率和带宽也增大,如图3(b)、(c)所示。在700 mW和800 mW激光能量下,加工的FBG的最大反射率分别为14.3 dB和15 dB,对应的带宽分别为0.62 nm和0.74 nm。这主要是由于越大的激光能量引起的折射率调制深度和有效折射率也越大,因此耦合效率增加,反射率增加,同时带宽也增加。另外,FBG达到最大

反射率所需要的曝光时间与激光能量的关系如图3(d)所示。可见激光能量越大,达到最大反射率所需的时间越短。在400 mW激光能量下,达到最大反射率所需的曝光时间大约为350 s,而800 mW激光能量条件下只需要6 s。拟合曲线表明,激光能量和曝光时间之间的变化关系是非线性的,两者可以完美使用指数函数拟合,拟合度高达0.9994。综上所述,在过大的激光能量下,虽然可以得到具有较大反射率的光栅,且曝光时间缩短,器件加工效率得到提高,但是带宽会显著增加。因此,在实际加工中应兼顾加工效率和光谱质量,激光能量不宜过小,也不宜过大。另外,评价FBG光谱质量的重要指标是其反射率的大小。根据式(2)可知,光栅的反射率主要取决于折射率调制量和光栅长度。对于相位掩模法获得的FBG,其光栅长度由掩模板和光纤之间的距离决定。激光能量变化会在光纤芯层中直接诱导产生不同的折射率调制量,从而导致反射率的变化;曝光时间的增加使得光纤的平均有效折射率增加,也会导致耦合效率的增加,从而影响光栅的反射率。但是在曝光时间达到一定值后,光栅反射率随曝光时间的变化并不显著,而激光能量的增加可以显著提高光栅的反射率。但是过大的激光能量会使光谱的旁瓣增多,带宽增大,光谱质量变差。此外,过大的激光能量也会增加掩模板的损伤。因此,在实际加工中,一般不会为了增加反射率而牺牲光谱质量,应该

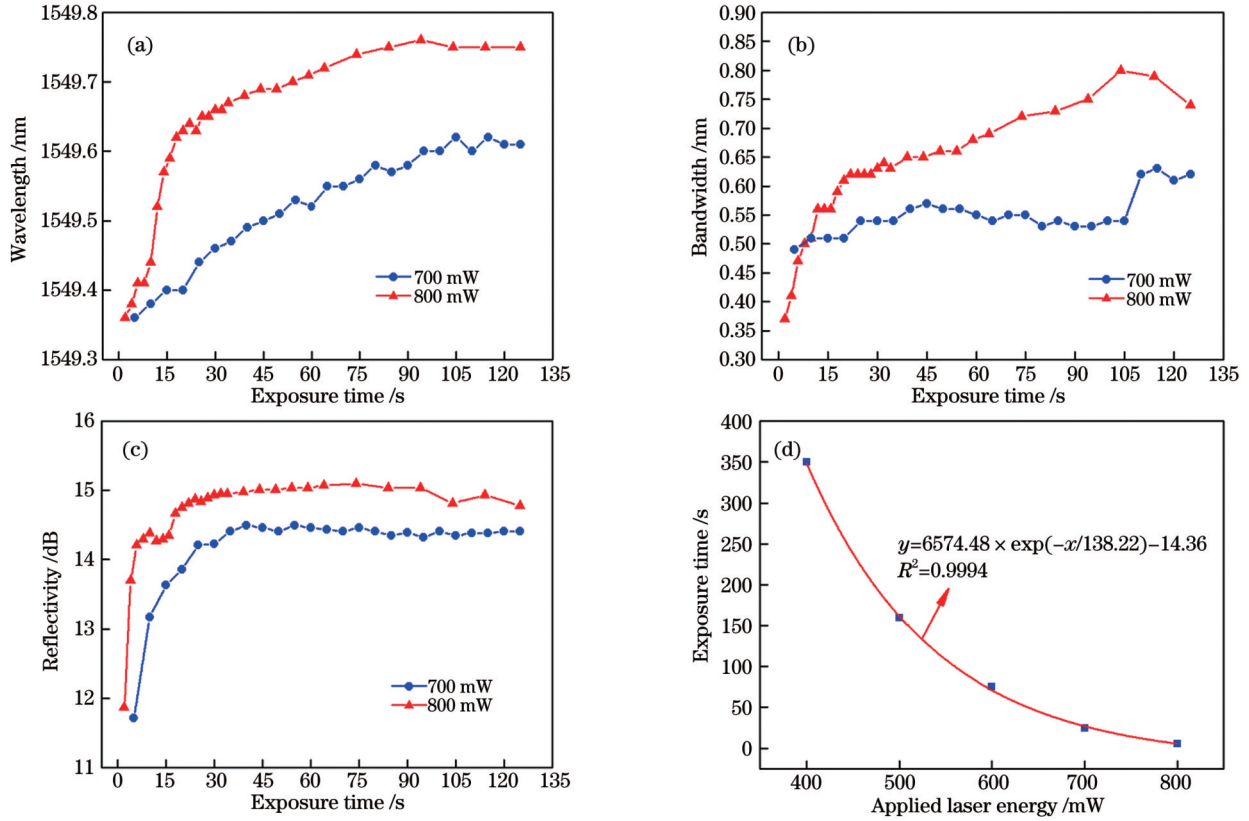


图3 激光能量对FBG反射光谱的影响。(a)波长、(b)反射率、(c)带宽随曝光时间的变化;(d)达到最大反射率所需的曝光时间与激光能量的关系

Fig. 3 Influence of laser energy on FBG reflectance spectrum. (a) Wavelength, (b) reflectivity, and (c) bandwidth versus exposure time; (d) relationship between applied laser energy and required exposure time to achieve maximal reflectivity

避免过大的激光能量,兼顾加工效率和光谱质量,选择激光能量和曝光时间的最优匹配。在本实验中,可以通过增大光栅长度和折射率调制量来提高反射率。为了增大光栅长度,可以减小光纤和掩模板的距离或者更换掩模板;为了增大折射率调制量,可以选择焦距更小的透镜,增强对光的聚焦能力。

图4所示为不同工艺条件下FBG的反射光谱。可以看出,当激光能量较大时,FBG主谐振峰两边会出现明显的旁瓣。

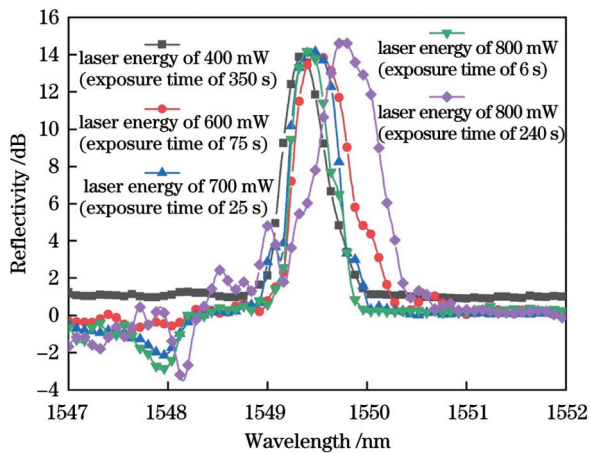


图4 不同工艺条件下FBG的反射光谱

Fig. 4 Reflection spectra of FBGs under different process conditions

出现明显的旁瓣。当激光能量为400 mW时,未见旁瓣,光谱主谐振峰两端光滑平坦;当能量大于600 mW时,主谐振峰左端出现明显旁瓣。这主要是由于较大的激光能量引起的折射率调制量和有效折射率的变化量较大,而激光光束是近似高斯光束,其能量分布服从正态分布,中间部分的激光能量相对较强,两端激光能量相对较弱,引起的折射率调制量的变化是不均匀的,且这种不均匀性在激光能量越大时越显著,因此激光能量较大时主谐振峰两端会产生明显旁瓣。此外,可以发现,短波方向上旁瓣的振荡显著而长波方向平顺。这是由于激光光束引起的折射率分布是高斯中心区域大而边缘小,中心区域诱导波长向长波方向的移动较向短波方向的多,从而填补了长波方向区域的“空隙”,因此长波方向相对平坦,而短波一侧振荡显著。通过光谱分析可知,在较大的能量下虽然会获得相对高的反射率,但是光谱带宽会变大、光谱主谐振峰的边缘质量也会变差,这些是不利于光纤传感的。因此,为了获得高质量的光谱,应该选择合适的激光能量,避免过大激光能量。

4 结 论

采用飞秒激光相位掩模法加工了FBG器件,搭建

了激光加工系统,重点研究了激光能量和曝光时间对 FBG 反射光谱的影响规律,分析了其波长、反射率和带宽的变化规律。实验发现,为了获得光谱质量好、带宽小、反射率大的 FBG 器件,需要选择合适的激光能量,激光能量不宜过大(不宜大于 800 mW)。在兼顾加工效率的前提下,激光能量在 600 mW 左右,曝光时间控制在 1 min 以内可获得较优效果。研究结果为优化加工参数提供了重要的实验依据。

参 考 文 献

- [1] Hill K O, Fujii Y, Johnson D C, et al. Photosensitivity in optical fiber waveguides: application to reflection filter fabrication[J]. *Applied Physics Letters*, 1978, 32(10): 647-649.
- [2] 王伟利, 延凤平, 张鲁娜. 基于多通道 FP-FBG 的波长可切换单纵模掺铥光纤激光器[J]. *中国激光*, 2021, 48(21): 2101001.
Wang W L, Yan F P, Zhang L N. Wavelength-switchable single-longitudinal-mode thulium-doped fibre laser with multi-channel FP-FBG[J]. *Chinese Journal of Lasers*, 2021, 48(21): 2101001.
- [3] 李亦佳, 王正方, 王静, 等. 基于光纤布拉格光栅振动传感器和极限学习机的工字钢梁损伤识别[J]. *中国激光*, 2021, 48(16): 1610004.
Li Y J, Wang Z F, Wang J, et al. Damage identification of I-beam based on fiber Bragg grating vibration sensor and extreme learning machine[J]. *Chinese Journal of Lasers*, 2021, 48(16): 1610004.
- [4] Sahota J K, Gupta N, Dhawan D. Fiber Bragg grating sensors for monitoring of physical parameters: a comprehensive review[J]. *Optical Engineering*, 2020, 59(6): 060901.
- [5] Liu Y C, Badcock R A, Fang X Y, et al. Selecting of FBG coatings for quench detection in HTS coils[J]. *IEEE Transactions on Applied Superconductivity*, 2018, 28(4): 9500305.
- [6] Liu Y C, Mataira R, Badcock R, et al. Application of epoxy-bonded FBG temperature sensors for high-temperature superconductor-coated conductor quench detection[J]. *IEEE Transactions on Applied Superconductivity*, 2021, 31(2): 4700308.
- [7] 廖常锐, 何俊, 王义平. 飞秒激光制备光纤布拉格光栅高温传感器研究[J]. *光学学报*, 2018, 38(3): 0328009.
Liao C R, He J, Wang Y P. Study on high temperature sensors based on fiber Bragg gratings fabricated by femtosecond laser[J]. *Acta Optica Sinica*, 2018, 38(3): 0328009.
- [8] Ghosh C, Priye V. Highly sensitive FBG strain sensor with enhanced measurement range based on higher order FWM[J]. *IEEE Photonics Journal*, 2020, 12(1): 6800407.
- [9] Wang J, Peng G D, Hu Z L, et al. Design and analysis of a high sensitivity FBG accelerometer based on local strain amplification [J]. *IEEE Sensors Journal*, 2015, 15(10): 5442-5449.
- [10] Ahmed F, Ahsani V, Saad A, et al. Bragg grating embedded in Mach-Zehnder interferometer for refractive index and temperature sensing[J]. *IEEE Photonics Technology Letters*, 2016, 28(18): 1968-1971.
- [11] Gouveia C, Jorge P A S, Baptista J M, et al. Fabry-Pérot cavity based on a high-birefringent fiber Bragg grating for refractive index and temperature measurement[J]. *IEEE Sensors Journal*, 2012, 12(1): 17-21.
- [12] Xu X Z, He J, He J, et al. Slit beam shaping for femtosecond laser point-by-point inscription of high-quality fiber Bragg gratings [J]. *Journal of Lightwave Technology*, 2021, 39(15): 5142-5148.
- [13] Yang K M, Liao C R, Liu S, et al. Optical fiber tag based on an encoded fiber Bragg grating fabricated by femtosecond laser[J]. *Journal of Lightwave Technology*, 2020, 38(6): 1474-1479.
- [14] Przhialkovskii D V, Butov O V. High-precision point-by-point fiber Bragg grating inscription[J]. *Results in Physics*, 2021, 30: 104902.
- [15] Zheng Y, Yu H H, Guo H Y, et al. Analysis of the spectrum distortions of weak fiber Bragg gratings fabricated in-line on a draw tower by the phase mask technique[J]. *Journal of Lightwave Technology*, 2015, 33(12): 2670-2673.
- [16] Qiu Y, Sheng Y L, Beaulieu C. Optimal phase mask for fiber Bragg grating fabrication[J]. *Journal of Lightwave Technology*, 1999, 17(11): 2366.
- [17] Meltz G, Morey W W, Glenn W H. Formation of Bragg gratings in optical fibers by a transverse holographic method[J]. *Optics Letters*, 1989, 14(15): 823-825.
- [18] Wang J, Lin C P, Liao C R, et al. Bragg resonance in microfiber realized by two-photon polymerization[J]. *Optics Express*, 2018, 26(4): 3732-3737.
- [19] Smelser C W, Mihailov S J, Grobnc D. Formation of Type I-IR and Type II-IR gratings with an ultrafast IR laser and a phase mask [J]. *Optics Express*, 2005, 13(14): 5377-5386.
- [20] Gattass R R, Mazur E. Femtosecond laser micromachining in transparent materials[J]. *Nature Photonics*, 2008, 2(4): 219-225.
- [21] Jia X S, Chen Y Q, Liu L, et al. Combined pulse laser: reliable tool for high-quality, high-efficiency material processing[J]. *Optics & Laser Technology*, 2022, 153: 108209.
- [22] Vengsarkar A M, Lemaire P J, Judkins J B, et al. Long-period fiber gratings as band-rejection filters[J]. *Journal of Lightwave Technology*, 1996, 14(1): 58-65.
- [23] Grobnc D, Smelser C W, Mihailov S J, et al. Long-term thermal stability tests at 1000 °C of silica fibre Bragg gratings made with ultrafast laser radiation[J]. *Measurement Science and Technology*, 2006, 17(5): 1009-1013.
- [24] Li Y H, Liao C R, Wang D N, et al. Study of spectral and annealing properties of fiber Bragg gratings written in H₂-free and H₂-loaded fibers by use of femtosecond laser pulses[J]. *Optics Express*, 2008, 16(26): 21239-21247.
- [25] Erdogan T. Fiber grating spectra[J]. *Journal of Lightwave Technology*, 1997, 15(8): 1277-1294.
- [26] 饶云江, 王义平, 朱涛. 光纤光栅原理及应用[M]. 北京: 科学出版社, 2006: 111-117.
Rao Y J, Wang Y P, Zhu T. Principle and application of fiber grating[M]. Beijing: Science Press, 2006: 111-117.
- [27] Kogelnik H. Filter response of nonuniform almost-periodic structures[J]. *The Bell System Technical Journal*, 1976, 55(1): 109-126.
- [28] Fertein E, Przygodzki C, Delbarre H, et al. Refractive-index changes of standard telecommunication fiber through exposure to femtosecond laser pulses at 810 nm[J]. *Applied Optics*, 2001, 40(21): 3506-3508.

Reflection Spectral Characteristics of Bragg Gratings Fabricated via Femtosecond Laser Phase Mask Technique

Dong Xinran¹, Wang Zian¹, Zeng Li^{2,3}, Sun Xiaoyan^{2,3*}

¹College of Mechanical and Electrical Engineering, Central South University of Forestry and Technology, Changsha 410018, Hunan, China;

²State Key Laboratory of High Performance Complex Manufacturing, College of Mechanical and Electrical Engineering, Central South University, Changsha 410083, Hunan, China;

³State Key Laboratory of High Performance Complex Manufacturing, Central South University, Changsha 410083, Hunan, China

Abstract

Objective Fiber Bragg gratings (FBGs) exhibit the advantages of small size, reflection operation, high sensitivity, and wavelength encoding. Further, the FBGs induced by femtosecond laser pulses have unique advantages, such as high-temperature resistance and high-temperature stability, which are particularly suitable for sensing applications under extreme operating conditions, and thus, these FBGs have been widely used in aerospace and other fields. Fabricating FBGs via phase mask technology has the merits of effective processing and high device consistency and has been demonstrated to be the most promising industrial technology scheme. However, limited research has been conducted on the spectral characteristics of FBGs. We fabricate FBGs via the femtosecond laser phase mask method and extensively study the influence of laser energy and exposure time on the wavelength, reflectivity, and bandwidth of the FBGs. The factors influencing the FBG spectrum are theoretically and experimentally analyzed. This study offers an experimental basis and guidance for the fabrication of high-quality FBG devices using femtosecond laser technology.

Methods In this study, FBGs fabricated via the femtosecond laser phase mask method are experimentally demonstrated. The light path of the grating processing system comprises a femtosecond laser system, aperture, optical attenuator, cylindrical lens, and phase mask. The spectrum testing system comprises an amplified spontaneous emission (ASE) broadband light source and an optical fiber spectrum analyzer. The laser system outputs 800 nm femtosecond laser pulses. A diaphragm and optical attenuator are used to control the spot diameter and adjust the laser pulse energy, respectively. Meanwhile, a cylindrical lens is used to focus the light beam, and a phase mask to form interference fringes and periodic structures in the fiber, and writing the gratings. In addition, a spectral testing system is used to monitor the spectral changes of the FBG in real time. In the experiment, when the laser energy is set to 600 mW and the longest exposure time is set to 240 s, the influence of exposure time on the FBG reflection spectrum is studied. Moreover, the relationship between the spectral properties and exposure time is analyzed under laser energy values of 700 mW and 800 mW.

Results and Discussions The influence of the exposure time on the FBG reflection spectrum is as follows. As shown in Fig. 2(a), when the exposure time increases, the FBG reflectivity gradually increases and then remains unchanged, and the wavelength undergoes a red shift. At the initial exposure time of 20 s, the FBG reflectivity reaches 11.6 dB rapidly, and then, at the exposure time of 75 s, reaches a maximum of approximately 14.03 dB, as shown in Fig. 2(b). Meanwhile, the bandwidth of the FBG increases with the exposure time, which increases from 0.41 nm to 0.73 nm in the exposure timer ange of 5–240 s, as displayed in Fig. 2(c). The FBG wavelength has a red shift as the exposure time increases and the wavelength changes by 0.36 nm, from 1549.33 nm to 1549.69 nm, as the exposure time increases from 5 s to 240 s, as shown in Fig. 2(d).

The influence of laser energy on the FBG reflection spectrum is as follows. As shown in Fig. 3(a), the higher the laser energy, the greater the red shift of the wavelength at the same exposure time. The corresponding wavelength at the exposure time of 125 s is 1549.61 nm and 1549.75 nm for the laser energy of 700 mW and 800 mW, respectively. The higher the laser energy, the higher is the reflectivity; however, the bandwidth also increases significantly. The corresponding maximum reflectivity values of FBG under the two conditions are 14.3 dB and 15 dB, respectively, as shown in Fig. 3(b). Simultaneously, the corresponding bandwidths of approximately 0.62 nm and 0.74 nm are achieved, as shown in Fig. 3(c). In addition, a higher laser energy leads to more side lobes on both sides of the main resonant peak in the spectrum, as shown in Fig.4.

Conclusions In this paper, FBGs fabricated using the femtosecond laser phase-mask method are proposed. The effects of laser energy and exposure time on the wavelength, reflectivity, and bandwidth are studied. The experimental results demonstrate that to obtain FBGs with a small bandwidth, high reflectivity, and high spectral quality, appropriate laser energy and exposure time should be selected. In particular, the laser energy should not be considerably large. Considering the writing efficiency and reflection spectral quality, an excellent FBG device can be obtained by selecting the laser energy of approximately 600 mW and exposure time of less than 1 min.

Key words fiber optics; fiber Bragg grating; femtosecond laser; phase mask method; spectral properties; bandwidth